

# Optimizing Membrane Performance using Various Filler Materials in Membrane Fabrication for Enhancing Gas Separation Efficiency: A Review

Putri Nadhirah Roslin<sup>1</sup>, Sazlinda Kamaruzaman<sup>1,2,\*</sup>,  
Ili Syazana Johari<sup>1</sup> and Noorfatimah Yahaya<sup>3</sup>

<sup>1</sup>Department of Chemistry Faculty of Science, Universiti Putra Malaysia, Selangor 43400, Malaysia

<sup>2</sup>Department Natural Medicines and Product Research Laboratory, Institute of Bioscience, Universiti Putra Malaysia, Selangor 43400, Malaysia

<sup>3</sup>Department of Toxicology, Advanced Medical and Dental Institute, Universiti Sains Malaysia, Penang 13200, Malaysia

(\*Corresponding author's e-mail: sazlinda@upm.edu.my)

Received: 7 May 2024, Revised: 15 June 2024, Accepted: 23 June 2024, Published: 20 October 2024

## Abstract

The membrane technology has been receiving significant interest in both research and industrial applications, particularly in the separation of CO<sub>2</sub>/CH<sub>4</sub>. These methods, as published, aim to overcome the limitations of pure polymeric membranes and offer an alternative approach in separation techniques where membrane technology can overcome the constraints of conventional methods such as Solid Phase Extraction (SPE) and Liquid-Liquid Extraction (LLE). Fabricating membranes using fillers as adsorbents can enhance membrane separation performance due to their porous nature. Hence, the selection of suitable fillers is crucial to maximize membrane efficiency in separating analytes. This paper will review 3 types of fillers-metal-organic frameworks, carbonaceous nanomaterials and mesoporous molecular sieves-from various research papers published in recent years.

**Keywords:** Membrane technology, Gas separation, Metal-organic framework, Carbonaceous nanomaterials, Optimization

## Introduction

Sample pre-treatment techniques are vital in a chemical analysis, where this step is carried out to remove the matrix and/or for analyte pre-concentration in order to achieve the desired detection limits [1]. Hence, the analytical performance in terms of selectivity, sensitivity and accuracy can be improved [2]. LLE and SPE are the traditional techniques of sample pre-treatment. There are certain drawbacks to the LLE technique where it is time consuming, involves a multistage operation and uses a large amount of organic solvents which are toxic and expensive. Meanwhile, the SPE technique is proposed as a replacement of LLE techniques since it has advantages in terms of reduced analysis time and organic solvent consumption. However, the SPE technique can be expensive [3].

An interest in membrane technology is rising over the last decade in research and industrial applications. The application of membranes for gas separation in industry begins since Mosanto installed the 1<sup>st</sup> commercialised gas separation for H<sub>2</sub> separation in 1980. Up until now, the membrane technology has been widely used in industry. Membrane materials selection is the crucial part, where it functions as

selective barrier which permeate preferred chemical species. Due to broad research on novel membrane materials, there are 3 types of membrane materials, which are inorganic, polymeric and polymer/filler hybrid membranes.

Polymer materials like poly ether ketone (PEK) has been widely used, presently, due to its minimal cost, excellent thin-film processability, excellent mechanical strength and appealing separation performances. However, is found that polymer-based membrane has certain limitations such as poor thermal stability, bad definition of free volume, poor chemical stability and most probably will undergo intense plasticization, with only few of polymeric membranes show good performance for gas separation.

Inorganic membranes using MOFs and Zeolite as framework which have better thermal and chemical stability have been studied and proposed as an alternative material to overcome polymeric membrane limitations. Inorganic membrane using MOFs and Zeolite have better separation performances in terms of selectivity and permeability due to their pore systems, resistance towards plasticization, excellent mechanical and thermal stability. Prevention of full-scale commercialization of inorganic membrane is due to its limitations in terms of complex fabrication, poor reproducibility, high cost and brittleness of materials. Hence, the mixed matrix membrane (MMMs) was introduced to overcome the challenge. MMM preparation includes dispersion of organic/inorganic materials as fillers on the polymer as matrixes, where it is expected to be synergistic combination of the polymers processability and fillers separation performances. The keywords used to filter the journals to be included in the mini review were mixed matrix membrane, metal-organic framework, carbon materials as adsorbent fillers in MMM, selectivity and permeability studies of MMM. While, the year of the selected journals were selected between 2019 to 2024.

### **Membrane technology**

Over the last decade, researchers and the industry has been focusing on the technology of the membrane and being applied broadly in various aspect of processes. Membrane materials function as a selective barrier that can permeate specific chemical species [4]. In present day, polymer has been chosen as membrane bulk phase due to their minimal production cost, good thin-film processability, mechanical strength and separation performance.

PEK is one of the common materials used for ultrafiltration, and PEK have good mechanical properties due to the presence of benzene ring, while the presence of large numbers of ether bonds gives PEK a good toughness since ether bonds provide flexibility to the molecular chain. However, polymeric membrane has low permeability rate due to its hydrophobic properties, which is why organic and inorganic adsorbent filler is introduced into the polymer matrix [5].

Fillers such as metal-organic frameworks (MOFs), carbonaceous materials, mesoporous silica and zeolites is introduced into polymer as an approach to overcome the limitations of polymeric membrane. The increasing trends of using doped nanoparticles or adsorbent filler, fused onto the polymer matrix is to improve the membrane hydrophobicity, contamination resistance, surface charge or pore size and porosity of the membrane. But this modification leads to membrane performance and stability trade-off [5]. The selection of fillers must be based on some critical factors, which can contribute to membrane performances, such as surface chemistry, chemical structure, aspect ratio and particle size distribution.

## **Materials and methods**

### **Materials for MMMs fabrication**

#### ***MOFs based-MMM***

Metal-organic framework (MOFs) are one of the best hybrid porous materials, which suitable for the MMMs fabrication. They are composed of nodes of inorganic materials linked by polytopic organic linkers

through bond of coordination (**Figure 1**) [6]. MOF possess some amazing properties such as structure diversity, abundant chemical functionalities, appealing porosities and tuneable pore structures, making them applicable for various applications such as gas storage and separation, catalysis and delivery [7]. Furthermore, the MOFs are much more excellent fillers in MMMs than the inorganic frameworks such as the zeolites. The “polymer-filler” interactions of the MOFs and the polymer chains of the matrix can be enhanced through the improved affinity between the polymer chains of the matrix and the organic linkers present in the MOFs. This helps in taking care of the nonselective voids or defects formation at the interface [7]. **Figure 1** below shows the chemical structure of 2 types of MOF group and its 3D model.

The purpose of using MOF fillers in the preparation of membranes is to utilize MOF unique properties in terms of diffusion and adsorption, hence enhancing both selectivity and permeability of the membrane. The main metrics in selecting MOF are based on its porosity, pore size and shape, functionality and tunability to different particle size and shape [7,8]. There are an abundance of MOFs having different porosity, however it is said that there is almost to none of specific and or systematic literature work about the effect of porosity on the permeability/selectivity trade-off. If the direct relationship between porosity and gaseous diffusive properties should be considered, MOF intrinsic porosity has a major role on the performances of MOF-based MMM. Therefore, if a specific polymer shows faster gas diffusion compared to MOF particles, then the particles will not be suitable to be used in MMM fabrication because the gas will be forced to use the fastest path [9].

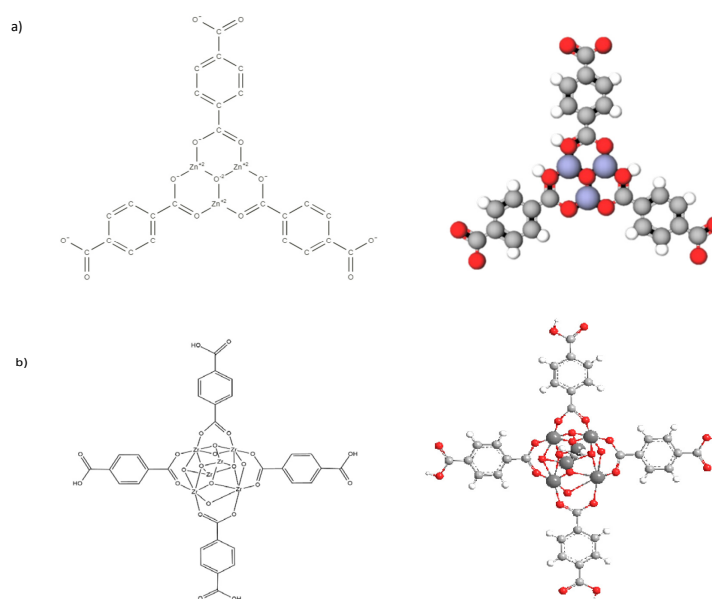


**Figure 1** The chemical structure and model of MOF: (a) MOF-5 and (b) UiO-66.

In order to achieve strong interaction between MOF and polymer, there 2 important issues that needs to be controlled. The 1<sup>st</sup> issue is that the separation performance of MOF can be affected by the non-selective voids formed due to aggregation of polymer and weak interfacial interactions between MOF and polymer matrices. Fabrication of MOF composites, MOF surface modifications and reducing the size of MOF nanocrystals are the solutions to improve interfacial compatibility between MOF and polymer matrix. The 2<sup>nd</sup> issue is to intensify functionalization of MOF, which include metal site modification, pore structure modulation, construct hydrogen-bonding acceptors and modification of functional ligand [10].

The defect-engineering of MOF crystal structure has gained attentions since the defects contribute to increase in porosity and forming numerous open metal site, which affect MOF adsorption capacity [10]. Lee *et al.* [11], synthesized a defective UiO-66 MOF by forming Zr-olefin complexes, and exhibit great separation performances on  $C_3H_6/C_3H_8$ .

Cui *et al.* [10] then proposed an approach by utilizing sodium formate modulated UiO-66 and  $NH_2$ -UiO-66 as fillers incorporated on polyetherimide (PEI) for MMM construction to separate  $CO_2/CH_4$ . The experiments were carried out with 3 different loadings of Zr-MOF powder, ranged from 5 to 20 wt% for both chosen fillers. Based on the SEM and TEM image of UiO-66 synthesized by [10], there are cubic crystals formed with size range from 150 to 200 nm. Modulation of both UiO-66 and  $NH_2$ -UiO-66 MOF with sodium formate successfully altered the particle size to 20 and 5 nm nanocrystals.

The single gas separation performances of UiO-66-ref-PEI, UiO-66-mod-PEI and  $NH_2$ -UiO-66-mod-PEI were carried out by Cui *et al.* [10]. The modulated Zr-MOF show higher  $CO_2$  permeability and  $CO_2/CH_4$  selectivity compared to UiO-66-ref-PEI. Larger crystal size of UiO-66-ref tends to aggregate and non-selective voids appear due to the failure of forming homogenous distribution resulting from the aggregation, hence lower the  $CO_2/CH_4$  selectivity. The negative effect of interfacial voids can be minimized by reducing the particle size, which is successfully achieved in this research. Sodium formate modulation on Zr-MOF able to inhibit the aggregation of nanoparticles.

The gas separation performance on different loadings (wt%) were demonstrated in this research, showing that 10 wt% of fillers have the optimum and highest value in  $CO_2$  permeability and  $CO_2/CH_4$  selectivity. However,  $CH_4$  permeability increases with the loadings. Higher amount of MOF can create higher free volume, and reducing the effective membrane thickness, enhancing the performance of the membrane [12].  $NH_2$ -UiO-66-mod-PEI shows better membrane performances than UiO-66-mod-PEI membrane due to the functionalization of amino group to Zr-MOF, which the amino group have higher affinity towards  $CO_2$ , and promotes  $NH_2$ -UiO-66-mod-PEI to have higher  $CO_2$  adsorption [10].

There is another study focused on the fabrication of 2 types of Zr-MOF, which are UiO-66 and MOF-808 onto PIM-1 mixed matrix membrane. Both of them have carboxylate-type linkers and Zr clusters, forming highly porous framework. Having advantages in ability to incorporate different various types of linkers making this MOF able to tailor its interaction with the polymer phase, affecting the gas transport properties of the MMM [13,14]. Various studies have examined that MOF have isorecticular chemistry properties, which the organic or inorganic of the reticular materials can be replaced without destroying the underlying structure [15], and reported that modified MOF for instance, functionalization of UiO-66 with  $-NH_2$  can affect and enhance their  $CO_2$  permeability and selectivity [16].

In this study, they proposed to synthesised MOF through microwave-assisted synthesis method by substituting dimethylformamide (DMF) with acetone and water with the reaction being carried on at low temperature. The membrane was fabricated with UiO-66 and MOF-808 as fillers with loadings ranging from 2.5 - 10 wt%. As reported in the paper, incorporation of both MOF particles has significant impact on permeability of  $CO_2$  and  $CO_2/CH_4$  selectivity. While, in comparison of UiO-66 and MOF-808 separation performance, MOF-808 shows better  $CO_2$  permeability rate due to its larger porosity and PIM 1-MOF-808 have higher selectivity value compared to PIM 1-UiO-66 [14], indicating that porous framework able to facilitate the gas diffusion rate, as well improving the membrane performances on gas permeability [16,17].

This conclude that the membrane can be optimized and maximized its separating efficiency by the following factors: 1) Reducing the particle size of the crystal particles to have better filler dispersion in the polymer matrix, mitigating the formation of non-selective voids. 2) Presence of defect sites, which in this research, achieved by addition of modulator sodium formate as capping agents [10].

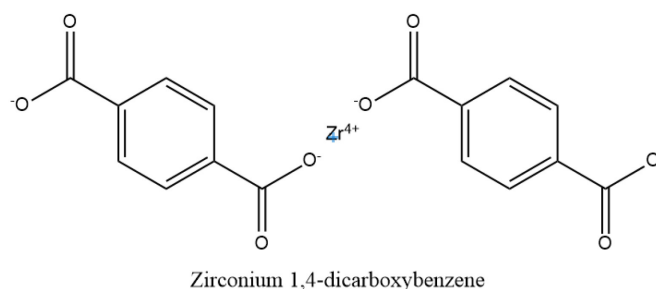


**Figure 2** UiO-66 building block chemical structure.

**Figure 2** shows the zirconium building block known for UiO-66. Zirconium (IV)-carboxylate MOF have strong hard acid-hard base coordination bonds between  $Zr^{4+}$  and carbonyl group, which gives it chemical and aqueous stability [5]. Electrostatic potential and acid-base lewis interactions within Zr-MOF carboxylate ligands contributed to exceptional performances, exhibiting good  $CO_2/CH_4$  permeability and selectivity [18,19]. This research has fabricated mixed matrix membrane using polymer of intrinsic microporosity (PIM) as polymer matrices, and the chosen fillers for this study are UiO-66 and MOF-808. Both are types of Zr-based MOF [14].

Functionality alterations in the pore network was studied to achieve these targets: 1) To enhance interactions between component to be separated and adsorbents and 2) To reduce pore size. Generally, the purpose of altering functionality of MOF is to boost selectivity-permeability trade-off [21]. **Table 1** shows various types of functionalities used for MOFs. As we can see from the table below, UiO-66 is the common MOF type being used as MMM fabrication.

UiO-66 is a common MOF having high surface area and high thermal stability. The metal oxide node is cuboctahedral, having 12 identical vertices allowing 12 extensions point, which then contributed to the stability properties. Besides, UiO-66 possess some other unique properties such as high stability in terms of mechanical, thermal, acidic, aqueous and water vapor. Due to its overall stability and porosity, UiO-66 is able to perform in aqueous applications [8].

**Table 1** The fabrication of MMM using MOF as fillers and its adsorption studies.

Adsorbent	Modification	Analyte	Adsorbent loading (wt%)	Characterization	Permeability and selectivity	Adsorption conditions	Remarks	Ref.
Zirconium MOF (UiO-66)	Addition of sodium formate for modulated UiO-66, membrane functionalized with $-NH_2$	$CO_2$ from separation of $CO_2/CH_4$	10 wt%	Zr-MOF formed in cubic crystal Crystal size (before modulation): 150 - 200 nm Crystal size (after modulation): 20 nm Crystal size (addition of $-NH_2$ group): 5 nm	Permeability UiO-66-mod-PEI: 395.6 barrer NH <sub>2</sub> -UiO-66-mod-PEI: 436.7 barrer Both membrane have the same selectivity: 46.8	$CO_2/CH_4$ gas feeding: 50/50 mL/min at 1 bar Membrane purge with Argon gas: 40 mL/min	$CH_4$ permeance rate rising with increasing MOFs loadings. Increase in MOF content leads to increasing of free volume, affecting the reduction in membrane thickness	[10]
Zirconium MOF (UiO-66 and MOF-808)		$CO_2$ from separation of $CO_2/CH_4$	10 wt%	Pristine PIM BET SSA: 728 $m^2/g$ MOF-808-PIM BET SSA: 738 $m^2/g$	$CO_2$ permeabilities increase with fillers loadings	Membrane surface area: 2.12 $cm^2$ Membrane temperature: 35 °C $CO_2/CH_4$ gas	Both PIM-1 and MOFs have small pore sizes and high BET SSA values.	[14]

Adsorbent	Modification	Analyte	Adsorbent loading (wt%)	Characterization	Permeability and selectivity	Adsorption conditions	Remarks	Ref.
				UiO-66-PIM BET SSA: 318 m <sup>2</sup> /g	(range 2.5 - 10 wt%) MOF-808-PIM: 8052 - 9090 barrer UiO-66-PIM: 7842 - 8995 barrer Selectivity MOF-808-PIM: 8.1 - 16.2 UiO-66-PIM: 8.1 - 12.5	feeding: 50/50 cm <sup>3</sup> (STP)/min at 3 bar Membrane permeate side purged at 1 bar with 2 cm <sup>3</sup> (STP)/min of He	BET SSA value for microwave synthesis MOF-808 lower than expected value. MOF-808-PIM have better permeability and selectivity value than UiO-66-PIM.	
NU-1000	NU-1000-PES MMM fabricated with graphene nanosheets (GNs)	H <sub>2</sub> /CO <sub>2</sub> , H <sub>2</sub> /NH <sub>2</sub> and H <sub>2</sub> /CH <sub>4</sub> separation	10 wt% NU-1000 0.03 wt% GNs		PES-0.03 % GNs- 10 % NU-1000 showing best results Gas permeabilities CO <sub>2</sub> : 365 barrer N <sub>2</sub> : 476 barrer H <sub>2</sub> : 1761 barrer CH <sub>4</sub> : 553 barrer PG3N have higher selectivity at 20 °C H <sub>2</sub> /CO <sub>2</sub> : 5 H <sub>2</sub> /N <sub>2</sub> : 4.2 H <sub>2</sub> /CH <sub>4</sub> : 3.3	Feeding gas temperature: (20 - 60) °C Feed pressure: 1 bar Membrane surface area: 2.88 cm <sup>2</sup>	Incorporation of GNs and Nu-1000 in MMMs shows excellent performance on gas separation. The permeability for all mixed gas stream increases with GNs loadings. The selectivity of PG3N increase 40, 23 and 57 %, respectively	[22]
UiO-66 MOF	UiO-66 MOF functionalized with amine group (-NH <sub>2</sub> )			FTIR and PXRD for the stretching vibrations of sulfonate groups and confirmation of MOF particles, respectively. Contact angle Pristine PES: 80 ° Sulfonated PES (SPES): 59.2 ° (reduced 26 % from PES). UiO-66-NH <sub>2</sub> /PES MMM: 44 ° for 5 wt% and 34.7 ° 10 wt%			Pure water flux and rejections for antifouling membrane test. Sulfonated membrane shows higher water flux compared to pristine PES. UiO-66-NH <sub>2</sub> have higher water flux compared to UiO-66 membrane, more hydrophilic property Pristine PES: 162.4 LMH SPES: 432.6 LMH UiO-66-NH <sub>2</sub> /SPES MMM: 665.5 LMH (5 wt%) and 678.0 LMH (10 wt%)	[23]
UiO-66 MOF	UiO-66 MOF functionalized with amine group (-NH <sub>2</sub> )	CO <sub>2</sub> , CO <sub>2</sub> /CH <sub>4</sub> binary feed	UiO-66 14 wt% UiO-66-NH <sub>2</sub> 16 wt%		Effect of CO <sub>2</sub> feed CO <sub>2</sub> permeability decreased 9 % for pristine 6FDA-DAM and 22 % for	Effect of CO <sub>2</sub> feed 20 bar, 35 °C, CO <sub>2</sub> content feed varies between 10 to 50 vol%	CO <sub>2</sub> permeability decreases with increasing CO <sub>2</sub> partial pressure when	[1]

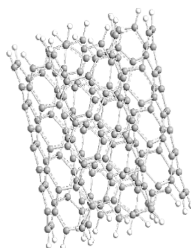
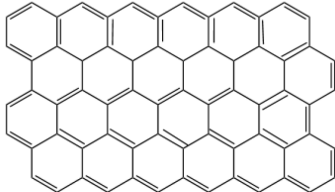
Adsorbent	Modification	Analyte	Adsorbent loading (wt%)	Characterization	Permeability and selectivity	Adsorption conditions	Remarks	Ref.
			UiO-66-NH-COCH <sub>3</sub> 16 wt%		Zr-MOF MMM. Effect of operating temperature increase in CO <sub>2</sub> permeance < 6 %, CH <sub>4</sub> permeance 28 and 37 %	Effect of operating temperature 30:70 vol% CO <sub>2</sub> :CH <sub>4</sub> feed mixture, 20 bar, 35 to 55 °C. Effect of H <sub>2</sub> S 30:70 vol% CO <sub>2</sub> :CH <sub>4</sub> feed mixture, 20 bar, 35 °C, 5 vol% H <sub>2</sub> S	tested at high pressure feeding. Presence of H <sub>2</sub> S reduced the CO <sub>2</sub> permeability due to active site on MOF have higher affinity towards H <sub>2</sub> S	
UiO-66 MOF	UiO-66 MOF functionalized with amine group (-NH <sub>2</sub> )			Contact angle decreases with increasing amount of MOF, reduced from 73.25 to 55.8 °  SEM to differentiate surface morphology, increasing amount of MOF leads to higher surface roughness	Pure water permeance increases from M0 (241.725 LMH) to M2 as optimum membrane having highest water permeance (482.3 LMH) with BSA rejection remain 98.7 %		Substitution of organic ligands by amino groups lead to higher hydrophilicity of MOF/MMM.	[5]
MIL-101	Thiol functionalization of MIL-101 using cysteamine, expected to bond with Ag.  Ag NPs impregnated in MIL-101 forming Ag(I)-thiolate complex.	Carbon monoxide (CO), CO/N <sub>2</sub> separation	10 wt%	FTIR and XRD to validate the synthesis of MOF and fabrication of MMM.  XRD pattern shows changes in crystallinity after addition of thiol and impregnation of Ag  SEM and TEM to study the membrane surface morphologies. Two hundred nm Ag/MIL-101 seen to be uniformly dispersed within the polymer matrix	Pristine PGO (polymer membrane) exhibits CO permeance at 2.53 GPU with CO/N <sub>2</sub> selectivity is 1.6  CO permeance and CO/N <sub>2</sub> selectivity increases with Ag/MIL-101 loading in MMM  10 wt% is the optimal Ag/MIL-101 loadings having CO permeance of 30.7 GPU and CO/N <sub>2</sub> selectivity 11.8	constant-pressure/variable volume method  5 bar, 30 °C, CO <sub>2</sub> /N <sub>2</sub> feed 80:20, 60:40 and 50:50 mol% at flow rate 250 mL/min	CO permeance, CO/N <sub>2</sub> selectivity decreases at higher loading of 20 wt% probably due to agglomeration of excess Ag/MIL-101	[25]
MIL-140C, UiO-67		CO <sub>2</sub> , CO <sub>2</sub> /N <sub>2</sub> and CO <sub>2</sub> /CH <sub>4</sub> separation	10 wt%	Strong absorption band C-O-C from PGO copolymer have slight blue shifted when incorporated with both MOFs, indicate the	Pristine PGO CO <sub>2</sub> permeance of 889 GPU and CO <sub>2</sub> /N <sub>2</sub> and CO <sub>2</sub> /CH <sub>4</sub> selectivity of 31 and 15, respectively  MIL/PGO and UiO-		10 wt% is the optimal MOF loading, membrane performance gradually decreases with increasing MOF content	[26]

Adsorbent	Modification	Analyte	Adsorbent loading (wt%)	Characterization	Permeability and selectivity	Adsorption conditions	Remarks	Ref.
				weak interaction between copolymer and MOF	67/PGO permeability increase with MOF content in MMM		higher than 10 wt%.  CO <sub>2</sub> permeability slightly higher in MIL/PGO compared to UiO-67/PGO	
MIL-53 (Al)		pyridine	15 wt%	SEM analysis shows MIL-53 (Al) have irregular shapes, 1.8 μm in size. The surface roughness increases as MIL-53 (Al) incorporate into the polymer matrix  Contact angle for pristine PEBA/PVDF is 79.6 %  Contact angle for MIL-53 (Al) MMM increases up to 20 wt% MOF loadings, indicating MIL-53 (Al) is hydrophobic	15-MIL-53 (Al) shows better pyridine flux than pristine PEBA/PVDF  PEBA/PVDF flux: 143.5 g/m <sup>2</sup> h  15-MIL-53 (Al)/PEBA/PVDF: 226.9 g/m <sup>2</sup> h  Pyridine flux increase 58.1 %	0.5 wt% pyridine in aqueous solution, 65 °C		[27]

### ***Carbonaceous nanomaterials as additives in MMM***

Recent advancements on nanotechnology have caused a rising interest in nanomaterials due to its environmentally sustainable properties. Nanomaterials have been used in various applications such as energy production, contaminant sensing and water treatment. Carbon nanoparticles is a resourceful material that can improve treating polluted water [28]. Carbon has different orbital hybridization, hence capable in forming different chemical bonds with various orientations. Due to this reason, carbon can have different allotropic forms, either graphite or diamond and forming a various nanostructures known as graphene, carbon nanotubes, carbon fibres, fullerenes, onion and nanodiamond [29].

**Table 2** Summary of carbonaceous materials properties.

Carbon nanostructure	Dimensional system	Hybridization	Layer	Structure
Carbon nanotubes	Unidimensional	Sp <sup>2</sup>	Multilayer and monolayer	 
Graphene	2-dimensional	Sp <sup>2</sup>	Monolayer	

### ***Carbon nanotubes***

Carbon nanotubes (CNTs) are 1 dimensional nanomaterial which has great properties in terms of mechanical and thermal, and are classified into 2 types according to the number of walls, known as single-walled carbon nanotubes (SWCNTs) and multi-walled carbon nanotubes (MWCNTs). SWCNTs are graphite in a single cylinder shape with a diameter up to 1.5 nm. While, MWCNTs consists of more than 1-cylinder sheets with a distance of 0.35 nm between sheets and have bigger diameter in comparison to SWCNTs, which is between 2 to 100 nm. The presence of interlayer spaces in MWCNTs might act as adsorption sites for smaller molecules [30].

CNTs have gained significant attention in membrane research due to their exceptional properties, such as high surface area and adsorption capacity, as well as their unique permeability characteristics. They have been incorporated into polymer matrices to create mixed matrix membranes, aiming to enhance the adsorption and permeability performance of the membranes. These mixed matrix membranes have been extensively studied to investigate the adsorption and permeability behaviour of carbon nanotubes when incorporated in a polymer matrix. Various techniques have been employed to evaluate the adsorption capacity of carbon nanotubes in mixed matrix membranes, including isotherm studies and breakthrough experiments. Additionally, permeability studies have been conducted to assess the transport properties of gases and liquids through these membranes. The results of these studies have demonstrated that the addition of carbon nanotubes to the polymer matrix can significantly enhance the adsorption and permeability performance of the mixed matrix membranes. Their high surface area and adsorption capacity contribute to enhanced adsorption of molecules, while their unique permeability characteristics facilitate the transport of gases and liquids through the membranes with reduced resistance. Overall, the adsorption and

permeability studies of mixed matrix membranes incorporating carbon nanotubes have shown promising results, highlighting their potential for various applications including gas separation, water purification and drug delivery systems. These studies provide valuable insights into the fundamental mechanisms governing adsorption and permeability in mixed matrix membranes and pave the way for further optimization and development of these membranes for practical applications [31-36].

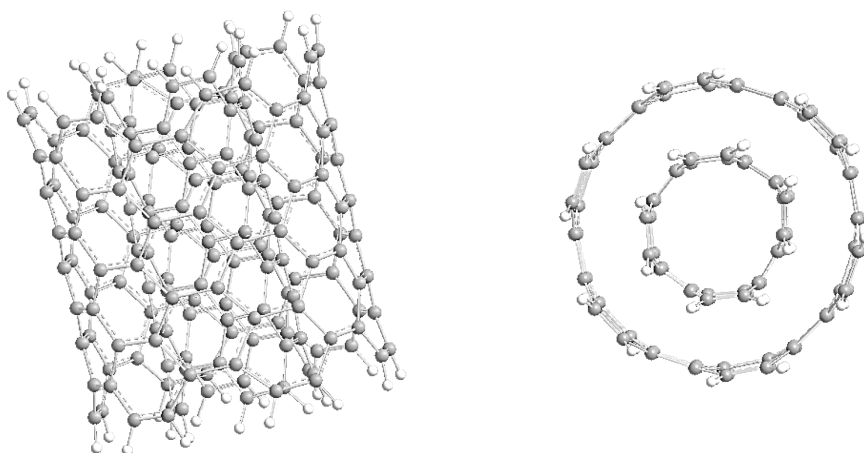


**Figure 3** Chemical structure of CNT.

CNTs have 1 issue which is, it tends to aggregate and this is causing the CNTs having poor interfacial interaction with polymer, affecting electrical and mechanical properties of the composite. CNTs surface functionalization is a common approach to solve this problem. Functionalization forming defect sites in CNTs affecting the degree of conjugation and reduce charge mobility [37-39]. Lee *et al.* [40] proposed and carried out a research of kinetic sorption studies on mixed matrix membrane CO<sub>2</sub>/N<sub>2</sub> separation, using cellulose acetate butyrate (CAB) as polymer matrix and MWCNTs as additives filler. In this study, the MMM was fabricated using wet inversion phase method, where the CAB polymers with 2 different molecular weight were mixed and added into functionalized MWCNTs (MWCNTs-F) for the dispersion of additives into the polymer matrix [40].

This study proposed to investigate if the difference in molecular weight (Mn) of CAB introduced into the doped solution of MWCNTs-F have significant impact on the enhancement of CO<sub>2</sub> adsorption behaviour. M1, M2 and M3 are membranes prepared with combination of CAB polymers at 70000:12000, 70000:30000 and 70000:65000, respectively, with a constant loading of MWCNTs-F, 0.8 wt%, with the objective to modify polymer chain packing while improving its properties, this work combines 2 polymers with varying Mn [41,42]. Single gas feeding to study the permeation rate of CO<sub>2</sub> and N<sub>2</sub> were carried out. As for CO<sub>2</sub> gas feeding, the permeation rate decreases with increasing molecular weight of CAB used in the membrane fabrication. Membrane thickness and composition are the factors affecting the permeance of CO<sub>2</sub>, where M1, having thin membrane thickness (8.34  $\mu\text{m}$ ), have the best permeation rate of CO<sub>2</sub> compared to M2 (8.45  $\mu\text{m}$ ) and M3 (9.8  $\mu\text{m}$ ). Acetyl group content, on the other hand, can influence the MMM's permeation ability; a low acetyl group concentration can slow down the gradually degrading densely packed entanglements, thereby promoting the membrane's capacity to adsorb CO<sub>2</sub>. Thus, M1 and M2 were able to attain high CO<sub>2</sub> permeance, but M3 had the lowest rate of CO<sub>2</sub> permeation while having the highest concentration of acetyl group [40-42].

As for N<sub>2</sub> permeance test, M1 able to attain higher N<sub>2</sub> into the membrane and the N<sub>2</sub> permeance decreases with the higher Mn of CAB polymer. This correlates to the higher intensity of carboxyl group (C=O) present in M2 and M3, where carboxyl group favoured in the adsorption of CO<sub>2</sub> while rejecting N<sub>2</sub>. Therefore, higher carboxyl group content in the membrane can create more sites for adsorption of CO<sub>2</sub>, consequently improving CO<sub>2</sub> permeability [40,43,44]. Contact angles analysis was conducted to study the N<sub>2</sub> permeance phenomena. The reduction in contact angles in M1 to M2 indicates that higher content of carboxyl group can improve the membrane hydrophilicity, where the end group -COOH cannot form hydrogen bond between polymer chains [45]. To assess the impact of polymer combination on mass transit between 2 penetrant gas molecules, the binary gas permeation investigation was continued in this study. The binary gas selectivity performance was evaluated at a ratio of 50/50 vol% for CO<sub>2</sub>/N<sub>2</sub> gas feeding. The ideal selectivity of binary gas mixture is lower than the pure single gas due to the low in CO<sub>2</sub> permeance because of the competitive permeation between the penetrant gases within the MMM [40]. In conclusion, the adsorption and permeability studies of mixed matrix membranes where carbon nanotubes are used as an adsorbent and incorporated in a polymer matrix have demonstrated enhanced adsorption and permeability performance, making them promising candidates for various applications [46,47].

### **Graphene**

Graphene, a 2-dimensional nanomaterial composed of a single layer of carbon atoms arranged in a honeycomb lattice structure, has gained significant attention in the field of membrane extraction [48]. The incorporation of graphene into polymeric matrix adsorption membranes has shown promise in improving the adsorption and permeability/selectivity properties for analytes removal or water treatment applications. Source: Graphene has been extensively studied for its unique properties and potential applications in various fields. Graphene's high surface area and exceptional mechanical properties enable it to effectively capture and remove contaminants from water and other fluids during membrane extraction processes. Furthermore, its excellent electron mobility contributes to enhanced adsorption and permeability/selectivity properties, making it an ideal material for improving the efficiency of analyte removal and water treatment applications [49,50].

Numerous studies have demonstrated the potential of graphene-enhanced membrane extraction in addressing key challenges in environmental remediation, industrial purification and water desalination. The unique properties of graphene offer promising opportunities for the development of advanced membrane technologies that can significantly improve the performance and sustainability of extraction processes [51]. Figure shows the difference in structure of graphene and carbon nanotubes.

A study was reported on the fabrication of ultra-thin polyether-block-amide (Pebax) MMM, where they used graphene oxide as additives for CO<sub>2</sub> capture [52]. GO has numerous oxygen-containing functional groups including ether (C-O-C), carboxyl (-COOH) and hydroxyl (-OH) groups. These functional group can form interaction with specific molecules through formation of hydrogen bonding and electrostatic interaction, that contributes to improvement of selectivity and separation of different molecules. This study chose Pebax as their polymer matrix, where it has the ability to interact with GO through hydrogen bonding, encouraging GO to assemble into a 2-dimensional laminated structure allowing for fast and selective transport pathways [53].

The fabrication of MMM in this study was carried out by coating GO/Pebax mixture on the surface of polydimethylsiloxane-block-polyethylene oxide/polyacrylonitrile (PDMS-PEO-PAN) membrane through knife casting method. Different membrane preparation conditions were evaluated to study the effects of it on the CO/N<sub>2</sub> separation performances. In this study, GO/Pebax acts as selective layer, while

PDMS-PEO is an intermediate layer [52]. Coating of GO/Pebax onto the surface of PDMS-PEO-PAN causing the membrane to increase in its surface roughness due to presence of GO nanosheets.

GO lateral size plays a crucial part in improving gas permeability and selectivity. Larger lateral size of GO will promote the stacking degree of GO since GO nanosheets will be arranged horizontally and increase transport resistance of gas molecules, consequently affecting the CO<sub>2</sub>/N<sub>2</sub> separation performances and membrane permeability and selectivity rate. Hence, this study proposed to use ultrasonic cell crusher, which is proven to reduce GO lateral size from 280 to 50 nm with increasing ultrasonic treatment time. Eventually, the lateral size reduction reached equilibrium at 4 h of treatment time. Separation performance test confirmed that the reduction in lateral size able to increase CO<sub>2</sub>/N<sub>2</sub> selectivity and CO<sub>2</sub> permeance by 12.5 and 70.2 %, respectively [52].

Then, they further the research by investigating the effect of GO nanosheets loadings on the surface roughness and how it can affect the GO/Pebax-MMM performances using SEM and AFM characterization. Based on their SEM results, membrane with less than 0.05 wt% have better dispersion and homogeneity, and the membrane tend to agglomerate when GO loadings is more than 0.075 wt%. As for AFM characterization, it can be concluded that the surface roughness increases with GO loadings. Even though theoretically increasing GO loadings meaning that the membrane can provide greater gas transport channels, GO can form a zig-zag transport pathways due to parallel stacking. As the GO loadings increases, CO<sub>2</sub>/N<sub>2</sub> selectivity shows significant improvement, however the CO<sub>2</sub> or N<sub>2</sub> permeance decreases. This can be explained through the thickness of the membrane which is 120 nm, so it is hard for the GO to be arranged vertically, and has to be stacked horizontally, increasing the gas molecules transport resistance [2]. This study successfully optimized the lateral size of GO nanosheets and GO content in MMM to achieve highest efficiency in CO<sub>2</sub> permeability and CO<sub>2</sub>/N<sub>2</sub> selectivity.

#### ***Effect of modified graphene***

Graphene is hydrophobic, hence adding suitable surfactants is an important step to obtain stable dispersions in polar solvents. Graphene oxide (GO) is the same as Graphene, despite the presence of oxygen-containing functional group (**Figure 4**). The presence of the functional group is to promote interaction and compatibility with polar solvents [54].

GO surface become negatively charged due to the presence of oxygen-containing functional groups, such as epoxy, carboxyl and hydroxyl. The structural properties of GO allow interaction with organic molecules via non-covalent forces like  $\pi - \pi$  stacking and hydrogen bonding [55]. Meanwhile, the adsorption process within the commercial graphene nanosheets is by low electrostatic interaction or Van Der Waals forces [56]. GO abundant oxygen-containing group and its regular laminar nanosheets is expected to provide fast and highly selective gas transport channel. It is reported that MMM containing GO as adsorbents have improve in terms of selectivity, however the permeability rate decreasing with increasing loading of GO into MMM. This effect can be attributed to the reduced mobility of polymer chain [57].

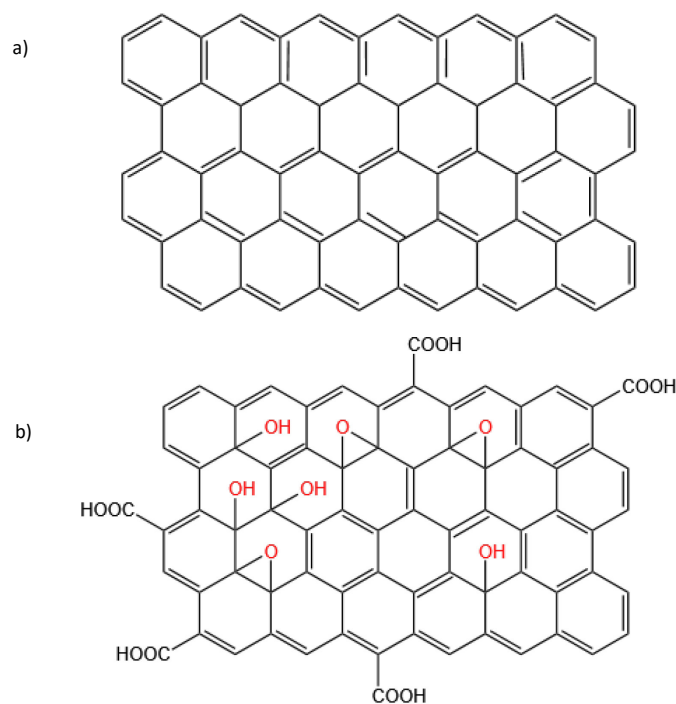


**Figure 4** Chemical structure of: (a) Graphene and (b) Graphene oxide.

#### ***Effect of graphene on MMM***

Incorporated of nanomaterials onto the MMM affects the membrane properties. The sizes of mean pore of MMM dispersed with adsorbents is higher compared to clean membranes. Specifically, this research carried out by comparing with 2 different fabrications. From the paper, it can be concluded that the mean pore size of MMM with MHNTs increase with higher loading of the adsorbents. However, this trend cannot be seen in MMM with GO as adsorbents. The mean pore size of the membranes showing decreasing in pattern as the loading of GO increased, which probably due to agglomeration of GO and strong hydrogen bonds between PVP and GO [55].

The presence of nanomaterials as adsorbents in the polymer matrix can increase the hydrophilic properties of the membrane. The changes in hydrophilic properties can be attributed to the hydrophilic nature of GO due to the presence of epoxy, carboxyl, or hydroxyl groups. Hence, increasing the loading of adsorbents can decrease the contact angle of the membranes, therefore, hydrophilic properties increase.

The presence of nanomaterial adsorbents increases the porosity of the membrane compared to pristine membranes. However, according to Amid *et al.* [58], increase loading of nanomaterials onto the membranes shows a reduction trend in membrane porosity. Despite increasing hydrophilicity properties in the membrane, it can cause adverse effect on uniform dispersion of adsorbents on the polymer, which then reduced the membrane porosity. Addition of nanomaterials in polymer can improve the tensile strength of the membrane. However, heavy loading of adsorbents onto the polymer matrix can decrease its tensile strength due to the agglomeration of GO in the polymer matrix. **Table 3** below shows the varies of research conducted on MMM using carbonaceous nanomaterials as additives/adsorbent fillers for various applications.

**Table 3** The fabrication of MMM using carbonaceous materials as fillers and its adsorption studies.

Adsorbent	Adsorbent modification	Target analyte	Adsorbent loading (wt%)	Characterization	Permeability and selectivity	Adsorption conditions	Remarks	Ref.
CNT	Functionalized with titanium oxide/TiO <sub>2</sub>	CO <sub>2</sub> , CO <sub>2</sub> /N <sub>2</sub> and CO <sub>2</sub> /CH <sub>4</sub> separations	0.5 wt%	FTIR spectra for PU/CNT-TiO <sub>2</sub> 3300 cm <sup>-1</sup> (-NH group stretching) 2870 and 2950 cm <sup>-1</sup> (symmetry and assymetry CH <sub>2</sub> absorption), 1125 cm <sup>-1</sup> (C-O-C absorption), 1700 and 1740 cm <sup>-1</sup> (free carbonyl group absorption)  XRD patterns exhibits a dominant amorphous halo at 2θ = 16.2 °  FESEM image shows good interaction between polymer matrix and CNT-TiO <sub>2</sub> , smooth surface	CO <sub>2</sub> have highest permeability rate compared to N <sub>2</sub> and CH <sub>4</sub> at optimum CNT loading (0.5 wt%, 49.12 barrer)  CO <sub>2</sub> permeance increases with CNT loadings, however the permeability dropped if CNT content > 0.5 wt%  CO <sub>2</sub> /N <sub>2</sub> have better selectivity, reaching highest value (55.82 barrer) with 0.5 wt% CNT	Various loadings of CNT@TiO <sub>2</sub> -2 (0, 0.25, 0.5, 0.75 and 1 wt%), pressures (4, 8 and 12 bar), temperatures (298, 308, 318 and 328 K)	TiO <sub>2</sub> functional groups provide better interfacial interaction between CNT and polymer base  Both permeability and selectivity increases with CNT loadings, optimized at 0.5 wt%. CNT loadings greater than 0.5 wt% leads to decrease in permeability and selectivity performances	[59]
MWCNT	Modify with EDA functionalization	CO <sub>2</sub> , CO <sub>2</sub> /N <sub>2</sub> separation	p-MWCNT (2.5 wt%) o-MWCNT (2.5 wt%) f-MWCNT (7.5 wt%)	Pristine MWCNT FTIR 1730 (C=O) and 1110 cm <sup>-1</sup> (C-O) stretching vibrations  f-MWCNTS FTIR 1720 (C=O) and 1114 cm <sup>-1</sup> (C-O)  SEM images of membrane; smooth surface for pristine Cardo-PIM-1 membrane  Heterogenous agglomeration when p-MWCNT added into polymer base, surface is not smooth  f-MWCNTs agglomerate and heterogeneously distribute in the Cardo-PIM-1 matrix	Cardo-PIM-1 + 2.5 wt% p-MWCNTs; CO <sub>2</sub> permeability: (8.0 ± 0.40) × 10 <sup>3</sup> barrer N <sub>2</sub> permeability: (5.6 ± 0.28) × 10 <sup>2</sup> barrer CO <sub>2</sub> /N <sub>2</sub> selectivity: 14.3  Cardo-PIM-1 + 2.5 wt% o-MWCNTs; CO <sub>2</sub> permeability: (1.8 ± 0.09) × 10 <sup>4</sup> barrer N <sub>2</sub> permeability: (9.8 ± 0.49) × 10 <sup>2</sup> barrer CO <sub>2</sub> /N <sub>2</sub> selectivity: 18.4  Cardo-PIM-1 + 7.5 wt% f-MWCNTs; CO <sub>2</sub> permeability: (2.9 ± 0.15) × 10 <sup>4</sup> barrer N <sub>2</sub> permeability: (1.2 ± 0.06) × 10 <sup>3</sup> barrer CO <sub>2</sub> /N <sub>2</sub> selectivity: 24.2	25 °C, 1 atm, CO <sub>2</sub> /N <sub>2</sub> feed (1:1)	FTIR stretching vibrations for C=O and C-O groups shifted due to the presence of amide group  The presence of -OH, -COOH and -NH <sub>2</sub> on the surface of MWCNTs de-bundles the highly entangled MWCNTs, enhanced dispersion in polymer matrix	[60]
MWCNT	Functionalized the surface with carboxyl group by treating with H <sub>2</sub> SO <sub>4</sub> and HNO <sub>3</sub>	O <sub>2</sub> , O <sub>2</sub> /N <sub>2</sub> separation		FTIR spectra exhibits 4 main peaks; 3430 (-OH stretch), 1700 (C-O stretching) and 1585 (C-C stretching) cm <sup>-1</sup>  Tensile strength; M@f-MWCNT-5 (60.3 MPa), M@f-MWCNT-10 (70.2 MPa) FESEM image shows both	Pristine matrimid; O <sub>2</sub> permeability: 1.81 ± 0.32 barrer O <sub>2</sub> /N <sub>2</sub> selectivity: 5.89 ± 0.14 barrer  M@f-MWCNT-5; O <sub>2</sub> permeability: 1.77 ± 0.17 barrer O <sub>2</sub> /N <sub>2</sub> selectivity: 6.94 ± 1.6 barrer	Helium (He) and compressed air (O <sub>2</sub> /N <sub>2</sub> : 21/79, O <sub>2</sub> 99.8 % and N <sub>2</sub> 99.999 %), 35 °C, constant pressure	O <sub>2</sub> /N <sub>2</sub> selectivity enhanced by 14.5 - 31.6 % points (f-MWCNTS concentration ranging from 5 - 10 wt%)  chloromethylation and	[61]

Adsorbent	Adsorbent modification	Target analyte	Adsorbent loading (wt%)	Characterization	Permeability and selectivity	Adsorption conditions	Remarks	Ref.
				pristine matrimid and matrimid incorporated by f-MWCNT have smooth and uniform surface  Membrane average thickness; 53 $\mu\text{m}$	M@f-MWCNT-10; O <sub>2</sub> permeability: 2.87 $\pm$ 0.25 barrer O <sub>2</sub> /N <sub>2</sub> selectivity: 7.83 $\pm$ 1.39 barrer		quaternization of the Matrimid membrane increased O <sub>2</sub> /N <sub>2</sub> selectivity while decreasing O <sub>2</sub> permeability.	
MWCNT		Pb <sup>2+</sup> , Hg <sup>2+</sup> and Cd <sup>2+</sup>	0.3 wt%	PCNT-0 having 65.73 ° contact angle due to high hydrophobic properties of polymer. The contact angles is said to reduce with increasing MWCNT loadings.  PCNT-3 (0.3 wt% CNT) has the highest value of; water uptake: (70.32 $\pm$ 0.72) % Porosity: (50.93 $\pm$ 0.69) % Contact angle: (61.79 $\pm$ 1.98) °  SEM image shows the formation of macro void within the MMM.  AFM results indicates surface roughness increases with MWCNT content in MMM	Adsorption study shows prepared membrane have limited affinity towards heavy metal  PCNT-3 shows highest heavy metal rejection, and this rejection enhancement mainly due to the sieving mechanism	500 ppm lead nitrate and cadmium nitrate, 50 ppm mercuric chloride, pH balanced to 6 $\pm$ 0.2 with 0.1 M HCl/0.1 M NaOH solution, stirred up to 5 continuous days, 25 °C, 5 cm <sup>2</sup> active area	Enhanced permeability and good rejection ability with increasing the MWCNTs wt% on PPSU polymer.  PCNT-3 membranes were exhibited best heavy metal rejection results of > 98 % for Pb <sup>2+</sup> , > 76 % for Hg <sup>2+</sup> and > 72 % for Cd <sup>2+</sup> ions, respectively.	[62]
GO		toluene/n-heptane separation		FTIR; stretching vibration -OH (3000 - 3500 cm <sup>-1</sup> ) C-O stretching (1048 cm <sup>-1</sup> ) C-O-C stretching (1222 cm <sup>-1</sup> ) C=O (1725 cm <sup>-1</sup> )  FESEM; 1.5 wt% GO have uniform dispersion in polymer matrix 1.5 to 2 wt%, GO tends to agglomerate, defects in structure  Total flux permeate increase with GO content ranging from 0.5 to 1.5 wt%, permeation flux reduced at GO content > 1.5 wt%			GOs' high affinity for aromatic compounds, MMM selectivity increased by more than 139 % compared to the pure membrane (pervaporation study)	[63]
GO	Iron oxide (Fe <sub>3</sub> O <sub>4</sub> )		0.4 wt%	Fe <sub>3</sub> O <sub>4</sub> /GO-PSf MMM; Porosity: 76.35 %			Functionalized GO MMM (Fe <sub>3</sub> O <sub>4</sub> /GO-	[64]

Adsorbent	Adsorbent modification	Target analyte	Adsorbent loading (wt%)	Characterization	Permeability and selectivity	Adsorption conditions	Remarks	Ref.
				Pore size: 0.0347 $\mu\text{m}$ contact angle: 69.97 $^\circ$			PSf) have the maximum permeation flux (112.47 L/m <sup>2</sup> .bar) compared to pristine PSf MMM (51.82 L/m <sup>2</sup> .bar)	
				GO-PSf MMM; Porosity: 64.39% Pore size: 0.0333 $\mu\text{m}$ Contact angle: 69.16 $^\circ$			All prepared membrane shows high CR rejection (> 85%), due to higher negativity surface charge	

### Mesoporous molecular sieve- based MMM

Mesoporous molecular sieve (M41S series) was first found in 1992, where they synthesized by mixing surfactant, silicate and alkali. Mesoporous silica has ordered hexagonal pore structure, which benefited them by having unique properties such as mechanically and thermally stable, able to undergo chemical functionalization, have high surface area due to reactive silanol groups present and well-defined mesoporous array as well as having bigger pores [65,66]. Mesoporous silica has a good adhesion to the polymer matrix due to its mesoporosity allowing polymer to penetrate into the pores.

However, it was reported by [66], the gas transport properties of MCM-41 and MCM-48 based membranes are difficult to fabricate due to polymer rigidity and poor interaction between polymer and particle. Besides adding fillers like mesoporous silica to overcome disadvantages shown by pristine polymeric membrane, these limitations also leading to several methods have been developed in objective to improve adhesion and polymer-particle interaction, by modifying fillers surfaces, addition of block copolymer [67].

Since mesoporous silica is widely used as fillers in membranes fabrication [68], there are various studies have been carried out and reported, where most of the studies has modified the particles surfaces by adding functionalized group, resulted in better polymer-particle interaction, improvement in gas transport properties and increasing gas selectivity [69]. **Table 4** is compilations some of the mesoporous silica-based membrane reported studies.

**Table 4** Compilations of reported studies on molecular sieve-based MMM.

Method	Mesoporous materials	Polymer	Functional derivatives	Application	Ref.
MMM	SBA-15	PES	Curcumin (Cur)	Zn <sup>2+</sup> , Pb <sup>2+</sup> and Ni <sup>2+</sup> removal	[70]
MMM	MCM-41	PSF	Amine	He, CO <sub>2</sub> , O <sub>2</sub> , N <sub>2</sub> and CH <sub>4</sub> separation	[71]
MMM	MCM-41	PSF	Pyrazole	CO <sub>2</sub> separation	[69]
MMM	MSS	Polyimide matrimid	-	CO <sub>2</sub> adsorption	[66]
MMM	Silica nanoparticles	Polyimide matrimid	-	ethylene/ethane and propylene/pyrene separation	[67]

As mentioned in the table above, a research study has been carried out to study the performance of MMM on removal of metal ions such as  $Zn^{2+}$ ,  $Pb^{2+}$  and  $Ni^{2+}$ . In this study, a new mesoporous material, Curcumin (Cur) modified mesoporous SBA-15 is chosen as filler incorporated into the PES polymer matrix for MMM fabrication. According to the authors, mesoporous Cur-SBA-15 have a significant impact on the removal of the targeted metal ions. The results obtained shows an improvement in its hydrophilicity, porosity, surface smoothness and antifouling ability.

**Figure 3** (reference to the research paper) represents the evaluation of antifouling properties of the membranes. The filtration experiments are conducted between the neat membrane and Cur-SBA-15 MMM using 8000 mg/L When milk solution is replaced by deionized water, the permeated flux of all investigated membranes decreases significantly, suggesting membrane fouling. On the other hand, modified mesoporous materials MMMs are found to have higher permeated flux compared to the neat polymeric membrane.

The authors also presented the heavy metal rejection by the prepared membranes, where the permeated flux and heavy metal rejections are evaluated using different concentration feeds (20, 50 and 60 mg/L), choosing M-0.3 membrane as the optimal modified membrane. Based on the graphs presented, it indicates that Cur-SBA-15 have higher rejection in compared to the neat membrane, and the membrane rejection reached maximum point when the mesoporous silica concentration is at 0.3 wt%. This is due to the hydrophilic nature of the modified MMM which play an important role of the membrane rejections.

#### ***Hybrid modifiers-MOF and carbonaceous material***

A study has been carried out to study the effect of using 2 different modifiers in MMM fabrication on physicochemical and properties of the MMM. Multiwall carbon nanotubes (MWCNTs) exhibit unique structure and valuable features in water purification, such as large surface-to-volume ratio, porosity, can be easily modified, excellent chemical and mechanical stability. In current studies, researches have been mixing up 2 adsorbents by modifying MOF with MWCNT to enhance their hydrophilic properties and the membrane performance [72].

In this particular study, they were using the combination of carboxylated MWCNTs (MWCNT-COOH) and MIL-53(Al) and expected to have better dispersion of MIL-53(Al). The physicochemical properties, membrane separation performances and antifouling behaviour were investigated. The hybrid additives loaded up onto the polymer matrix at different weight by percentage, where reached the maximum total porosity at 88.36 % with 5 wt% of MIL-53(Al)@MWCNTs content in MMM. This indicates that the addition of MIL-53(Al)@MWCNTs creates more aggregates due to the formation of interfacial defects. From SEM images of the MMM, addition of MIL-53(Al) alone, at 5 wt% tends to self-accumulate in PES polymer matrix. Accumulation problems can affect the membrane performance. When compared to SEM image of hybrid MIL-53(Al)@MWCNTs at 5 wt%, it showed that the accumulation has improved since the combination able to improve the MOF distribution, preventing self-accumulation due to the presence of oxygen group in MIL-53(Al)@MWCNTs, increasing its compatibility with PES matrix [73].

The surface hydrophilicity correlates with membrane permeability and antifouling properties. Water contact angle (WCA) for pristine PES MMM is 62 ° and this value decreases as the number of additives loadings in MMM increases. PES/MIL-53(Al)@MWCNTs and PES/MIL-53(Al), both with 5 wt% loadings, have WCA value at 32 and 58 °, respectively. This indicates that MIL-53(Al) tailored with MWCNTs able to increase its hydrophilic properties due to the presence of carboxyl group within the nanocomposite, affecting the average pore radius and overall porosity of the membrane. Characterization studies from this research concluded that PES/MIL-53(Al)@MWCNTs at 5 wt% loading have the optimum condition and proceeded to test its performance [73].

The separation efficiency for the prepared and fabricated membrane shows 77 - 98 % removal efficiencies of dyes. It was reported by various studies that MIL-53(Al), PES membranes and MWCNT-COOH are negatively charged at pH 7. PES/MIL-53(Al)@MWCNTs at 5 wt% loading exhibit the highest removal efficiency for amoxicillin removal with the value of 93.07 %, which may be related with the interaction between carboxyl group from MIL-53(Al)@MWCNT-COOH with amine and hydroxyl group from amoxicillin [73].

The research findings on antifouling properties test that 3 parameters (pH, initial concentration and MWCNTs loading) can possibly affect the fouling properties of MMMs. The modified membrane having larger pore size, higher overall porosity and improved negative surface charged between pH 4 - 12. The membrane which contains 5 wt% of MIL-53(Al)@MWCNTs have highest permeation flux of 246.2 L/m<sup>2</sup>.h compared to the bare PES membrane. In conclusion, porosity and the presence of carboxyl group which affecting the hydrophilic properties of the membrane, can increase the membrane performances and efficiency in removing contaminants from wastewater [73].

### Conclusions

Mixed matrix membrane, a combination of polymeric matrix has been widely studied for its potential for membrane technology improvements, especially in terms of their permeability and selectivity. Metal-organic frameworks, carbonaceous nanomaterials, silica molecular sieve are the commonly used fillers among the other available fillers in the market due to their exceptional properties in mitigating the limitations from pure polymer membranes. MMM production is environment friendly and use less energy, which is important in producing a sustainable separation method. However, recent MMM research is only on the foundation level and there is no available framework based MMM produced on a commercial scale. In order to evaluate the membrane performances, these parameters must be considered; high pressure, high temperature and presence of plasticization in order to developed a MMM that are chemically and thermally stable.

### Acknowledgements

The authors gratefully acknowledge the financial support by Ministry of Education Malaysia (Fundamental Research Grant Scheme with the reference number of Ref: FRGS/1/2023/STG04/UPM/02/5).

### References

- [1] S Kamaruzaman, PC Hauser, MM Sanagi, WAW Ibrahim, S Endud and HH See. A simple microextraction and preconcentration approach based on a mixed matrix membrane. *Analytica Chimica Acta* 2013; **783**, 24-30.
- [2] Y Zhang, WE Zhou, JQ Yan, M Liu, Y Zhou, X Shen, YL Ma, XS Feng, J Yang and GH Li. A review of the extraction and determination methods of thirteen essential vitamins to the human body: An update from 2010. *Molecules* 2018; **23**, 1484.
- [3] F Augusto and ALP Valente. Applications of solid-phase microextraction to chemical analysis of live biological samples. *TrAC Trends Anal. Chem.* 2002; **21**, 428-38.
- [4] FN Al-Rowaili, M Khaled, A Jamal and U Zahid. Mixed matrix membranes for H<sub>2</sub>/CO<sub>2</sub> gas separation - A critical review. *Fuel* 2023; **333**, 126285.
- [5] Y Zhang, D Liu, Z Wang, J Yu, Y Cheng, W Li, Z Wang, H Ni and Y Wang. Amino-functionalized UiO-66-doped mixed matrix membranes with high permeation performance and fouling resistance. *Chin. J. Chem. Eng.* 2024; **67**, 68-77.

- [6] RJ Kuppler, DJ Timmons, QR Fang, JR Li, TA Makal, MD Young, D Yuan, D Zhao, W Zhuang and HC Zhou. Potential applications of metal-organic frameworks. *Coord. Chem. Rev.* 2009; **253**, 3042-66.
- [7] W Li, Y Zhang, Q Li and G Zhang. Metal-organic framework composite membranes: Synthesis and separation applications. *Chem. Eng. Sci.* 2015; **135**, 232-57.
- [8] J Winarta, B Shan, SM McIntyre, L Ye, C Wang, J Liu and B Mu. A decade of UiO-66 research: A historic review of dynamic structure, synthesis mechanisms, and characterization techniques of an archetypal metal-organic framework. *Cryst. Growth Des.* 2020; **20**, 1347-62.
- [9] M Vinoba, M Bhagiyalakshmi, Y Alqaheem, AA Alomair, A Pérez and MS Rana. Recent progress of fillers in mixed matrix membranes for CO<sub>2</sub> separation: A review. *Sep. Purif. Tech.* 2017; **188**, 431-50.
- [10] Y Cui, X Cui, G Yang, P Yu, C Wang, Z Kang, H Guo and D Xia. High CO<sub>2</sub> adsorption of ultra-small Zr-MOF nanocrystals synthesized by modulation method boosts the CO<sub>2</sub>/CH<sub>4</sub> separation performance of mixed-matrix membranes. *J. Membr. Sci.* 2024; **689**, 122174.
- [11] TH Lee, JG Jung, YJ Kim, JS Roh, HW Yoon, BS Ghanem, HW Kim, YH Cho, I Pinnau and HB Park. Defect engineering in metal-organic frameworks towards advanced mixed matrix membranes for efficient propylene/propane separation. *Angewandte Chemie Int. Ed.* 2021; **60**, 13081-8.
- [12] Z Tahir, M Aslam, MA Gilani, MR Bilad, MW Anjum, LP Zhu and AL Khan. SO<sub>3</sub>H functionalized UiO-66 nanocrystals in *Polysulfone* based mixed matrix membranes: Synthesis and application for efficient CO<sub>2</sub> capture. *Sep. Purif. Tech.* 2019; **224**, 524-33.
- [13] OG Nik, XY Chen and S Kaliaguine. Functionalized metal organic framework-polyimide mixed matrix membranes for CO<sub>2</sub>/CH<sub>4</sub> separation. *J. Membr. Sci.* 2012; **413-414**, 48-61.
- [14] M Yahia, LA Lozano, JM Zamaro, C Téllez and J Coronas. Microwave-assisted synthesis of metal-organic frameworks UiO-66 and MOF-808 for enhanced CO<sub>2</sub>/CH<sub>4</sub> separation in PIM-1 mixed matrix membranes. *Sep. Purif. Tech.* 2024; **330**, 125558.
- [15] Y Yang, P Fernández-Seriñán, I Imaz, F Gándara, M Handke, B Ortín-Rubio, J Juanhuix and D Maspoch. Isorecticular contraction of metal-organic frameworks induced by cleavage of covalent bonds. *J. Am. Chem. Soc.* 2023; **145**, 17398-405.
- [16] MR Khdhayyer, E Esposito, A Fuoco, M Monteleone, L Giorno, JC Jansen, MP Attfield and PM Budd. Mixed matrix membranes based on UiO-66 MOFs in the polymer of intrinsic microporosity PIM-1. *Sep. Purif. Tech.* 2017; **173**, 304-13.
- [17] DY Kang and JS Lee. Challenges in developing MOF-based membranes for gas separation. *Langmuir* 2023; **39**, 2871-80.
- [18] LS Lai, YF Yeong, KK Lau and MS Azmi. Zeolite imidazole frameworks membranes for CO<sub>2</sub>/CH<sub>4</sub> separation from natural gas: A review. *J. Appl. Sci.* 2014; **14**, 1161-7.
- [19] D Liu, Y Wu, Q Xia, Z Li and H Xi. Experimental and molecular simulation studies of CO<sub>2</sub> adsorption on zeolitic imidazolate frameworks: ZIF-8 and amine-modified ZIF-8. *Adsorption* 2013; **19**, 25-37.
- [21] B Achiou, M Karunakaran, MR Tchalala and Y Belmabkhout. *MOF mixed matrix membranes for CO<sub>2</sub> separation*. In: MR Rahimpour, M Farsi and MA Makarem. *Advances in carbon capture*. Woodhead Publishing, Cambridge, 2020, p. 331-55.
- [22] A Mohamed, S Yousef, V Makarevicius and A Tonkonogovas. GNs/MOF-based mixed matrix membranes for gas separations. *Int. J. Hydrogen Energy* 2023; **48**, 19596-604.
- [23] M Al-Shaeli, SJD Smith, S Jiang, H Wang, K Zhang and BP Ladewig. Long-term stable metal organic framework (MOF) based mixed matrix membranes for ultrafiltration. *J. Membr. Sci.* 2021; **635**, 119339.

- [24] MZ Ahmad, TA Peters, NM Konnertz, T Visser, C Téllez, J Coronas, V Fila, WMD Vos and NE Benes. High-pressure CO<sub>2</sub>/CH<sub>4</sub> separation of Zr-MOFs based mixed matrix membranes. *Sep. Purif. Tech.* 2020; **230**, 115858.
- [25] M Kang, KC Kim, SB Min, HJ Min, SY Lee, BR Park, JH Kim and JH Kim. Highly CO-selective mixed-matrix membranes incorporated with Ag nanoparticle-impregnated MIL-101 metal-organic frameworks. *Chem. Eng. J.* 2022; **435**, 134803.
- [26] M Kang, TH Kim, HH Han, HJ Min, YS Bae and JH Kim. Submicron-thick, mixed-matrix membranes with metal-organic frameworks for CO<sub>2</sub> separation: MIL-140C vs. UiO-67. *J. Membr. Sci.* 2022; **659**, 120788.
- [27] R Khan, WM Liu, IU Haq, HG Zhen, H Mao and ZP Zhao. Fabrication of highly selective PEBA mixed matrix membranes by incorporating metal-organic framework MIL-53 (Al) for the pervaporation separation of pyridine-water mixture. *J. Memb. Sci.* 2023; **686**, 122014.
- [28] A Raza, S Altaf, S Ali, M Ikram and G Li. Recent advances in carbonaceous sustainable nanomaterials for wastewater treatments. *Sustainable Mater. Tech.* 2022; **32**, e00406.
- [29] A Hirsch. The era of carbon allotropes. *Nat. Mater.* 2010; **9**, 868-71.
- [30] NH Mukhtar and HH See. Carbonaceous nanomaterials immobilised mixed matrix membrane microextraction for the determination of polycyclic aromatic hydrocarbons in sewage pond water samples. *Analytica Chimica Acta* 2016; **931**, 57-63.
- [31] HH Tseng, IA Kumar, TH Weng, CY Lu and MY Wey. Preparation and characterization of carbon molecular sieve membranes for gas separation-the effect of incorporated multi-wall carbon nanotubes. *Desalination* 2009; **240**, 40-5.
- [32] SM Sanip, AF Ismail, PS Goh, T Soga, M Tanemura and H Yasuhiko. Gas separation properties of functionalized carbon nanotubes mixed matrix membranes. *Sep. Purif. Tech.* 2011; **78**, 208-13.
- [33] AF Ismail, PS Goh, SM Sanip and M Aziz. Transport and separation properties of carbon nanotube-mixed matrix membrane. *Sep. Purif. Tech.* 2009; **70**, 12-26.
- [34] S Kim, TW Pechar and E Marand. Poly(imide siloxane) and carbon nanotube mixed matrix membranes for gas separation. *Desalination* 2006; **192**, 330-9.
- [35] PS Rao, MY Wey, HH Tseng, IA Kumar and TH Weng. A comparison of carbon/nanotube molecular sieve membranes with polymer blend carbon molecular sieve membranes for the gas permeation application. *Microporous Mesoporous Mater.* 2008; **113**, 499-510.
- [36] S Kim, L Chen, JK Johnson and E Marand. Polysulfone and functionalized carbon nanotube mixed matrix membranes for gas separation: Theory and experiment. *J. Membr. Sci.* 2007; **294**, 147-58.
- [37] H Li, W Choi, PG Ingole, HK Lee and IH Baek. Oxygen separation membrane based on facilitated transport using cobalt tetraphenylporphyrin-coated hollow fiber composites. *Fuel* 2016; **185**, 133-41.
- [38] N Preethi, H Shinohara and H Nishide. Reversible oxygen-binding and facilitated oxygen transport in membranes of polyvinylimidazole complexed with cobalt-phthalocyanine. *React. Funct. Polym.* 2006; **66**, 851-5.
- [39] S Harms, K Rätzke, F Faupel, N Chaukura, PM Budd, W Egger and L Ravelli. Aging and free volume in a polymer of intrinsic microporosity (PIM-1). *J. Adhes.* 2012; **88**, 608-19.
- [40] RJ Lee, ZA Jawad, HB Chua and AL Ahmad. Blend cellulose acetate butyrate/functionalised multi-walled carbon nanotubes mixed matrix membrane for enhanced CO<sub>2</sub>/N<sub>2</sub> separation with kinetic sorption study. *J. Environ. Chem. Eng.* 2020; **8**, 104212.
- [41] A Fakhar, M Sadeghi, M Dinari and R Lammertink. Association of hard segments in gas separation through polyurethane membranes with aromatic bulky chain extenders. *J. Membr. Sci.* 2019; **574**, 136-46.

- [42] ETS Wong, ZA Jawad, BLF Chin and SK Wee. A kinetic study of CO<sub>2</sub> sorption improvement in the CA-CNTs mixed matrix membrane. *In: Proceedings of the International Conference on Process Engineering and Advanced Materials*, Kuala Lumpur, Malaysia. 2018, p. 12066.
- [43] X Zhang, T Zhang, Y Wang, J Li, C Liu, N Li and J Liao. Mixed-matrix membranes based on Zn/Ni-ZIF-8-PEBA for high performance CO<sub>2</sub> separation. *J. Membr. Sci.* 2018; **560**, 38-46.
- [44] M Shan, Q Xue, N Jing, C Ling, T Zhang, Z Yan and J Zheng. Influence of chemical functionalization on the CO<sub>2</sub>/N<sub>2</sub> separation performance of porous graphene membranes. *Nanoscale* 2012; **4**, 5477-82.
- [45] A Rahimpour, M Jahanshahi, S Khalili, A Mollahosseini, A Zirepour and B Rajaeian. Novel functionalized carbon nanotubes for improving the surface properties and performance of polyethersulfone (PES) membrane. *Desalination* 2012; **286**, 99-107.
- [46] MN Nejad, M Asghari and M Afsari. Investigation of carbon nanotubes in mixed matrix membranes for gas separation: A review. *ChemBioEng Rev.* 2016; **3**, 276-98.
- [47] T Wang, JN Shen, LG Wu and BVD Bruggen. Improvement in the permeation performance of hybrid membranes by the incorporation of functional multi-walled carbon nanotubes. *J. Membr. Sci.* 2014; **466**, 338-47.
- [48] F Bonaccorso, A Lombardo, T Hasan, Z Sun, L Colombo and AC Ferrari. Production and processing of graphene and 2d crystals. *Mater. Today* 2012; **15**, 564-89.
- [49] Z Liu, W Wang, X Ju, R Xie and L Chu. Graphene-based membranes for molecular and ionic separations in aqueous environments. *Chin. J. Chem. Eng.* 2017; **25**, 1598-605.
- [50] N Song, X Gao, Z Ma, X Wang, Y Wei and C Gao. A review of graphene-based separation membrane: Materials, characteristics, preparation and applications. *Desalination* 2018; **437**, 59-72.
- [51] X Yu, L Wang, Z Xu, S Song, D Fu and G Zhang. Fabrication of graphene-based membranes for solvent-resistant nanofiltration. *IOP Conf. Ser. Earth Environ. Sci.* 2018; **170**, 52039.
- [52] F Yang, Y Jin, J Liu, H Zhu, R Xu, F Xiangli, G Liu and W Jin. Regulation of interlayer channels of graphene oxide nanosheets in ultra-thin Pebax mixed-matrix membranes for CO<sub>2</sub> capture. *Chin. J. Chem. Eng.* 2023; **67**, 257-67.
- [53] J Shen, G Liu, K Huang, W Jin, KR Lee and N Xu. Membranes with fast and selective gas-transport channels of laminar graphene oxide for efficient CO<sub>2</sub> capture. *Angewandte Chemie Int. Ed.* 2015; **54**, 578-82.
- [54] LKD Assis, BS Damasceno, MN Carvalho, EHC Oliveira and MG Ghislandi. Adsorption capacity comparison between graphene oxide and graphene nanoplatelets for the removal of coloured textile dyes from wastewater. *Environ. Tech.* 2020; **41**, 2360-71.
- [55] W Falath. Novel stand-alone PVA mixed matrix membranes conjugated with graphene oxide for highly improved reverse osmosis performance. *Arabian J. Chem.* 2021; **14**, 103109.
- [56] LA Chacra, MA Sabri, TH Ibrahim, MI Khamis, NM Hamdan, S Al-Asheh, M Alrefai and C Fernandez. Application of graphene nanoplatelets and graphene magnetite for the removal of emulsified oil from produced water. *J. Environ. Chem. Eng.* 2018; **6**, 3018-33.
- [57] S Quan, SW Li, YC Xiao and L Shao. CO<sub>2</sub>-selective mixed matrix membranes (MMMs) containing graphene oxide (GO) for enhancing sustainable CO<sub>2</sub> capture. *Int. J. Greenhouse Gas Control* 2017; **56**, 22-9.
- [58] X Cao, K Wang and X Feng. Incorporating ZIF-71 into poly(ether-block-amide) (PEBA) to form mixed matrix membranes for enhanced separation of aromatic compounds from aqueous solutions by pervaporation. *Sep. Purif. Tech.* 2022; **300**, 121924.
- [59] AM Norouzi, ME Kojabad, M Chapalaghi, A Hosseinkhani, AA Nareh and EN Lay. Polyester-based polyurethane mixed-matrix membranes incorporating carbon nanotube-titanium oxide coupled

- nanohybrid for carbon dioxide capture enhancement: Molecular simulation and experimental study. *J. Mol. Liq.* 2022; **360**, 119540.
- [60] H Sun, W Gao, Y Zhang, X Cao, S Bao, P Li, Z Kang and QJ Niu. Bis(phenyl)fluorene-based polymer of intrinsic microporosity/functionalized multi-walled carbon nanotubes mixed matrix membranes for enhanced CO<sub>2</sub> separation performance. *React. Funct. Polym.* 2020; **147**, 104465.
- [61] M Patil, SG Hunasikari, SN Mathad, AY Patil, CG Hegde, MA Sudeept, MK Amshumali, AM Elgorban, S Wang, LS Wong and A Syed. Enhanced O<sub>2</sub>/N<sub>2</sub> separation by QuaternizedMatrimid/multiwalled carbon nanotube mixed-matrix membrane. *Heliyon* 2023; **9**, e21992.
- [62] MC Nayak, AM Isloor, Inamuddin, B Lakshmi, HM Marwani and I Khan. Polyphenylsulfone/multiwalled carbon nanotubes mixed ultrafiltration membranes: Fabrication, characterization and removal of heavy metals Pb<sup>2+</sup>, Hg<sup>2+</sup>, and Cd<sup>2+</sup> from aqueous solutions. *Arabian J. Chem.* 2020; **13**, 4661-72.
- [63] M Pakizeh, M Karami, S Kooshki and R Rahimnia. Advanced toluene/n-heptane separation by pervaporation: Investigating the potential of graphene oxide (GO)/PVA mixed matrix membrane. *J. Taiwan Inst. Chem. Eng.* 2023; **150**, 105025.
- [64] PV Chai, E Mahmoudi, AW Mohammad and PY Choy. Iron oxide decorated graphene oxide embedded polysulfone mixed-matrix membrane: Comparison of different types mixed-matrix membranes on antifouling and performance. In: Proceedings of the International Conference on Sustainable Energy and Green Technology, Bangkok. 2020, p. 12174.
- [65] S Xu, C Zhou, H Fang, W Zhu, J Shi and G Liu. Synthesis of ordered mesoporous silica from biomass ash and its application in CO<sub>2</sub> adsorption. *Environ. Res.* 2023; **231**, 116070.
- [66] B Zornoza, C Téllez and J Coronas. Mixed matrix membranes comprising glassy polymers and dispersed mesoporous silica spheres for gas separation. *J. Membr. Sci.* 2011; **368**, 100-9.
- [67] SM Davoodi, M Sadeghi, M Naghsh and A Moheb. Olefin-paraffin separation performance of polyimide Matrimid<sup>®</sup>/silica nanocomposite membranes. *RSC Adv.* 2016; **6**, 2346-59.
- [68] M Rezakazemi, AE Amooghini, MM Montazer-Rahmati, AF Ismail and T Matsuura. State-of-the-art membrane based CO<sub>2</sub> separation using mixed matrix membranes (MMMs): An overview on current status and future directions. *Prog. Polym. Sci.* 2014; **39**, 817-61.
- [69] F Suhail, M Batool, T Anjum, AT Shah, S Tabassum, AL Khan, H AlMohamadi, M Najam and MA Gilani. Enhanced CO<sub>2</sub> separation performance of polysulfone membranes via incorporation of pyrazole modified MCM-41 mesoporous silica as a nano-filler. *Fuel* 2023; **350**, 128840.
- [70] G Moradi, S Zinadini, M Rahimi and F Shiri. Efficient Zn<sup>2+</sup>, Pb<sup>2+</sup>, and Ni<sup>2+</sup> removal using antifouling mixed matrix nanofiltration membrane with curcumin modified mesoporous Santa Barbara Amorphous-15 (Cur-SBA-15) filler. *J. Environ. Chem. Eng.* 2022; **10**, 107302.
- [71] S Kim and E Marand. High permeability nano-composite membranes based on mesoporous MCM-41 nanoparticles in a polysulfone matrix. *Microporous Mesoporous Mater.* 2008; **114**, 129-36.
- [72] J Cao, J Zhou, Y Zhang and X Liu. A clean and facile synthesis strategy of MoS<sub>2</sub> nanosheets grown on multi-wall CNTs for enhanced hydrogen evolution reaction performance. *Sci. Rep.* 2017; **7**, 8825.
- [73] MS Rostami and MM Khodaei. Investigation of permeability, hydrophilicity, and pollutant removal properties of PES/MIL-53(Al)@MWCNT nanofiltration membrane. *Chem. Eng. J.* 2023; **475**, 146074.